MONITORING ACOUSTIC EMISSIONS TO PREDICT MODULUS OF RUPTURE OF FINGER-JOINTS FROM TROPICAL AFRICAN HARDWOODS

Joshua Ayarkwa
Graduate Student

Yoshihiko Hirashima
Professor

Kosei Ando
Research Associate

and

Yasutoshi Sasaki
Associate Professor
Bio-material Engineering Laboratory
Graduate School of Bioagricultural Sciences
Nagoya University, Furo-cho, Chikusaku
Nagoya 464-8601, Japan

(Received July 2000)

ABSTRACT

The acoustic emission patterns generated from bending tests of finger-joints from three tropical African hardwoods, Obeche (*Triplochiton scleroxylon*), Makore (*Tieghemella heckelii*), and Moabi (*Baillonella toxisperma*) were evaluated to determine the possibility of using them to predict finger-joint modulus of rupture.

The patterns of acoustic emissions generated from the bending tests were observed to differ, depending on the type of finger profile and wood species. The regression coefficient of the regression of cumulative acoustic emission count on applied stress squared also varied with the profile and species type. When modulus of rupture was correlated with this regression coefficient, for stresses applied up to 50% of mean ultimate strength, the logarithmic regression model developed could predict modulus of rupture of the finger-joints accurately to ±10%, ±12%, and ±21% for Obeche, Makore, and Moabi, respectively. The models developed also seemed sensitive to the quality of the finger-joints from the three tropical African hardwoods.

The results of the study gave an indication that this acoustic emission monitoring procedure could be useful for nondestructively predicting modulus of rupture of finger-joints from the three tropical African hardwoods.

Keywords: Acoustic emission, finger-joints, tropical African hardwood, modulus of rupture.

INTRODUCTION

The need to set up finger jointing plants to efficiently utilize the enormous volume of trim ends and other lumber residues generated in sawmills in Ghana and other tropical lumber-producing African countries has been expressed several times (Prah 1994; Ofosu-Asiedu et al. 1996). This is not only an opportunity for a mill to upgrade waste and improve return on low-grade lumber, but also a means to promote the efficient utilization of tropical timber.

A finger-joint, which is a type of structural end joint, is said to be one of the most economic ways of wood utilization. By finger jointing, low-grade timber is used to produce

Wood and Fiber Science, 33(3), 2001, pp. 450–464

high quality finished products with improved strength and appearance through the removal of undesirable characteristics (Strickler 1980; Kohler 1981; Fisette and Rice 1988; Ulasovets and Makerova 1988; Beaulieu et al. 1997). According to Lembke (1977), finger-jointed studs commonly bring premium prices because they are straighter and dimensionally more stable than solid studs.

Although classic static tests are considered as more desirable evaluation methods for the mechanical properties of structural timber, they are sometimes difficult to perform and are time-consuming. Fast, reliable, and easy-to-use nondestructive methods for predicting finger-joint strength properties will not only offset the above difficulty, but also go a long way to promote the efficient utilization of mill residues. Nondestructive wood testing permits wood properties of individual timber pieces determined destructively to be correlated with other wood properties measured nondestructively in order to assign property values without damage due to overloading, thereby improving the efficiency of timber utilization (Bodig and Jayne 1982).

Acoustic Emissions

Creation of fracture surfaces in adhesive joints under load causes release of strain energy in the region of the advancing crack. This generates elastic waves, called acoustic emission (AE), created by sudden increases in defect size during the process of loading to failure (DeBaise et al. 1966; Noguchi et al. 1986; Suzuki and Schniewind 1987; Rice and Skaar 1990). Although AE originates with initial fracture, it is commonly considered nondestructive at that stage (Hartbower et al. 1972; Porter et al. 1972; Dedhia and Wood 1980; Ansel 1982). Dunegan and Harris (1968) were among the first to realize that the AE process could be developed into a valuable nondestructive test technique for structures or components of structures. According to Porter et al. (1972) and Knuffel (1988), fractures develop in three distinct phases: initiation, growth, and ultimate failure. In the opinion of the authors, it is useful to consider failure not as a single event in time but rather as a developing process, beginning with the first application of stress on a structure. According to the authors, for a heterogeneous material such as wood, one need not be concerned with this first stage of flaw initiation, as any large wood component will contain a number of potentially damaging inherent flaws. The second stage of the failure process is the flaw growth phase, in which some of the flaws continually increase in size until one of them reaches a critical size for the imposed stress condition, leading to ultimate failure-the sudden propagation of a crack through the structure. The authors reported that fracture growth in lumber commences at very low stress levels, increases slowly at first, and then at a certain point "takes off" rapidly, escalating in frequency and extent until failure takes place. Chistensen (1962) using relatively unsophisticated electronic equipment was able to detect small cracks growing at loads as low as 25% of failure stress, and currently AE activities in some materials can be observed at much lower stress levels using modern equipment. DeBaise et al. (1966) reported that the strain energy or stress waves released are, in most cases, caused by a shift in a local defect area, sometimes called micro-checks, and arise from local stress concentrations in nonhomogenous materials. Other known reasons for the production of AE include material dislocations, phase changes, or the growth of cracks (Rice and Skaar 1990). As a material is stressed, the resulting AEs produced at the defect site propagate throughout the material, and are usually detected by a sensor or transducer attached directly to the surface being monitored (Porter et al. 1972; Dedhia and Wood 1980; Honeycutt et al. 1985; Rice and Skaar 1990). The sensor converts the incoming signal to an electric impulse, which is amplified and conditioned to remove extraneous noise. Many systems in current use allow the emissions to be filtered such that only signals (termed "counts" or "event-counts") above a certain

TABLE 1. *Selected finger profiles for the finger-joints.*

Profile type	Finger length L (mm)	Pitch P (mm)	Tip width t (mm)	Slope of fingers θ	Relative joint area ($2L/p$)	Cross section reduction (t/p)
F1	10	3.7	0.6	1 in 6	5.5	0.16
F2	18	3.7	0.6	1 in 12	9.7	0.16
F3	20	6.0	0.6	3 in 20	6.7	0.10

Refer to Figure 1.

threshold level are registered (Rice and Skaar 1990). The most common method of reporting AE activity is to describe the count rate or cumulative event-counts as a function of the stress applied to the material (Rice and Skaar 1990).

Porter (1964) was the first to study the application of AE to wood, by using it in a study of fracture mechanics in wood. There have been several attempts at using the technique to evaluate the strength of adhesive bonds. The amount of strain energy released during failure is usually correlated with mechanical properties of the adhesive joints. Pollock (1971) used the technique to predict failure of adhesive bonds stressed in tension, and found that specimens with poor adhesion had a higher emission rate than those with good adhesion and began to emit at lower stress levels. Porter et al. (1972) and Dedhia and Wood (1980) used AE to predict failure of 2-in. × 6-in. (i.e., 50-mm × 150-mm) Douglas fir finger-joints and showed how the method could be used as a nondestructive testing method for wood. The studies indicated that prediction of the ultimate bending strength depended on the load at which the prediction was made and the nature of the finger-joint. Porter et al. (1972) reported that for normal commercial finger-joint stock, load level just beyond the proportional limit should permit estimates of failure load accurate to ±10%. Dedhia and Wood (1980) also concluded that the joint strength could be estimated at 80% of failure load with an accuracy of 7%. Sato et al. (1985) on the application of AE to mechanical testing of wood reported a useful regression of AE count on load squared. According to DeBaise et al. (1966) and Knuffel (1988), AE emission rate is affected by the type of loading, whether tension, bending, or compression.

The AE technique differs from other nondestructive tests in one important aspect. Usually the nondestructive engineer probes the component under test with some form of energy, and notes the existence of defects from the absorption of energy. In the AE method, the structure itself becomes an active participating test member, with the growing defects emitting energy, which is a reflection of the failure process itself.

The objective of the study was to determine whether the patterns of AE generated by the finger-joints from three tropical African hardwoods could well correlate with modulus of rupture (MOR) for nondestructively predicting the MOR.

MATERIALS AND METHODS

Materials

Finger-joints were prepared under factory conditions from three profile types (Table 1 and Fig. 1) using defect-free, straight-grained lumber samples of Obeche (*Triplochiton scleroxylon*) of mean density of 351 kg/m^3, Makore (*Tieghemella heckelii*) of mean density of 677 kg/m^3, and Moabi (*Baillonella toxisperma*) of mean density of 819 kg/m^3. The lumber samples were matched on the basis of their modulus of elasticity, determined by the longitudinal vibration technique, before jointing (Samson 1985; Fisette and Rice 1988). The joints were produced using weather-resistant, fully exterior resorcinol formaldehyde glue (DIANOL 33N) and were end-pressed with three different pressures (Table 2). The different finger profiles and end-pressures were

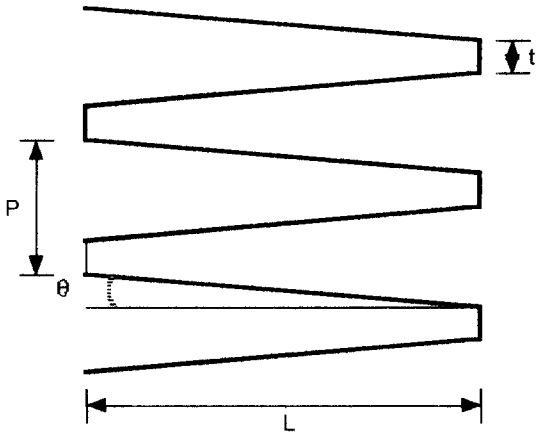

FIG. 1 Finger profile parameters.

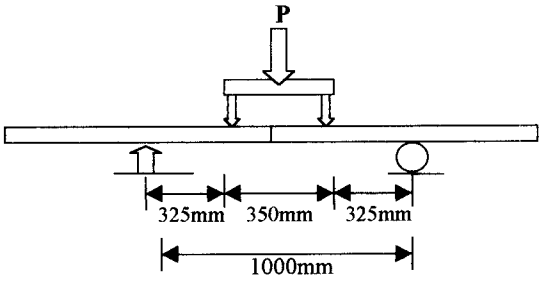

FIG. 2 Schematic diagram of set-up of bending test for finger-jointed specimens.

studied in order to secure a wide range of failure stresses for the analyses. Due to the low compressive strength of the wood of Obeche, end-pressures different from those studied for profiles F1 and F2 were studied for profile F3 (Table 2), to avoid excessive splits observed at the roots of the fingers of profile F3 during initial trial tests. The adhesive was double spread on the samples before pressing, and the specimens were cured under a temperature of 30°C for about 48 h. No pressure was applied to the specimens during curing. The samples were planed, ripped, and cross-cut to bending test specimen dimensions of 21 × 70 × 2000 mm for Makore and Moabi, and 21 × 58 × 2000 mm for Obeche, due to insufficient lumber samples of Obeche. Test specimens were conditioned to 10% moisture content, under controlled temperature of 20 ± 1°C and relative humidity of 55 ± 3%, before testing.

Static bending test

The bending specimens were tested using an INSTRON TCM 10000 test machine of static loading capacity of ±100 kN. Crosshead speeds of 20 mm/min (for Makore and Moabi) and 5 mm/min (for Obeche) were chosen, and failure occurred within 3 to 5 min of test duration (a compromise between duration specified by the JIS Z 2101 (1977) and ASTM D 198-84 [1994]). Each replication of specimen was tested under a four-point loading arrangement in accordance with the ASTM D 198-84 (ASTM 1994). The distance between the loads was 350 mm (Fig. 2). The total span tested for the finger-jointed specimen was 1000 mm. The specimen was positioned on the supports such that the finger-joint was at the center of the 1000-mm span. Deflection was measured within the shear-free zone using two transducers positioned at each side of the finger-joint. All the specimens were loaded to failure, and modulus of rupture (MOR), modulus of elasticity (MOE), and the proportional limit stress were calculated. Only specimens that failed at the finger-joints were considered

TABLE 2. *End-pressures for the finger-jointing (MPa).*

End-pressure	Timber species					
	Moabi and Makore			Obeche		
	F1	F2	F3	F1	F2	F3
P1		8		4	4	2
P2		12		8	8	3
P3		18		12	12	4

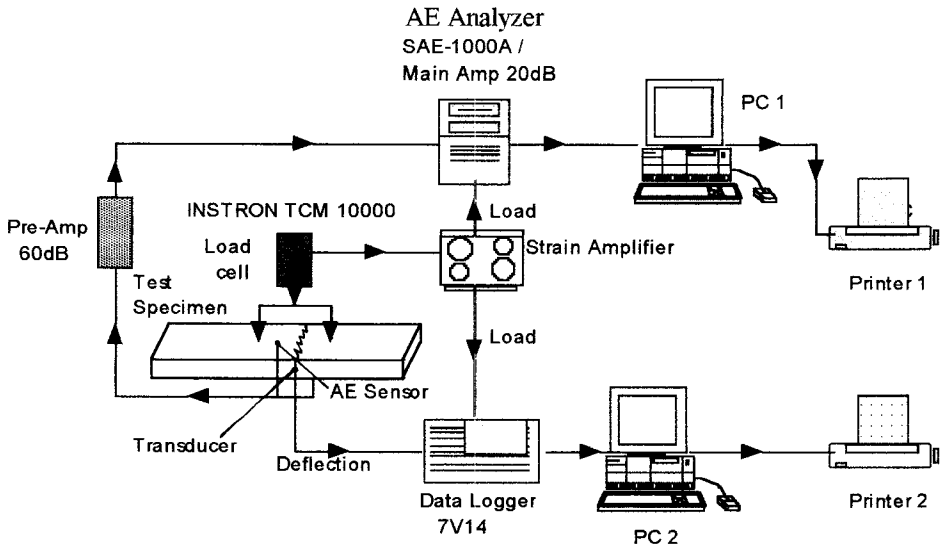

FIG. 3 Schematic diagram of the acoustic emission test set-up.

in the subsequent data analyses. Ten replications of finger-jointed specimens were tested for each combination of finger profile and end-pressure for each species, resulting in 90 specimens for each species.

Recording of acoustic emissions

Two AE sensors were coupled to each face of a test specimen 25 mm apart on each side of the finger-joint, with the aid of silicon grease and rubber bands (Figs. 2 and 3). Signals received by the AE sensors were preamplified to 40 dB and further amplified by a main-amplifier to 20 dB. Threshold level was 50 mV. This threshold was just above the noise level at the beginning of the test, and thus eliminated the possibility of introducing emission signals arising from changing background noise level. An AE Analyzer, model SAE-1000A, equipped with band filters received, filtered, and cumulatively counted the amplified signals (Fig. 3). The filters were set between 100 kHz (High Pass Filter) and 500 kHz (Low Pass Filter). All signals outside this band were attenuated. Loads were also channeled through a strain amplifier to the AE Analyzer. The digital signals from the counter were converted to analog form, and both loads and counts were sent to a personal computer for analysis.

Data analyses

Analyses of variance of test data from different end-pressure.—An attempt was made to increase sample size for the analyses by combining statistically similar data from the different end-pressures studied for each profile type for each species. Consequently, one-way analyses of variance (ANOVA) were performed using the F-test to verify whether MORs obtained from the different end-pressures of each finger profile type were the same. The test did not reject the null hypothesis at 5% significance level. The test data from the three end-pressures of each finger profile type were therefore combined and analyzed for each species.

Selection of stress levels for predicting MOR.—For nondestructive prediction of strength, low stress levels are desirable so as to not cause incipient failure in the finger-joints that would subsequently lead to failure in service, nor break too many samples being tested. The accuracy of predicting finger-joint strength, however, has been reported to decrease, the farther away from the ultimate

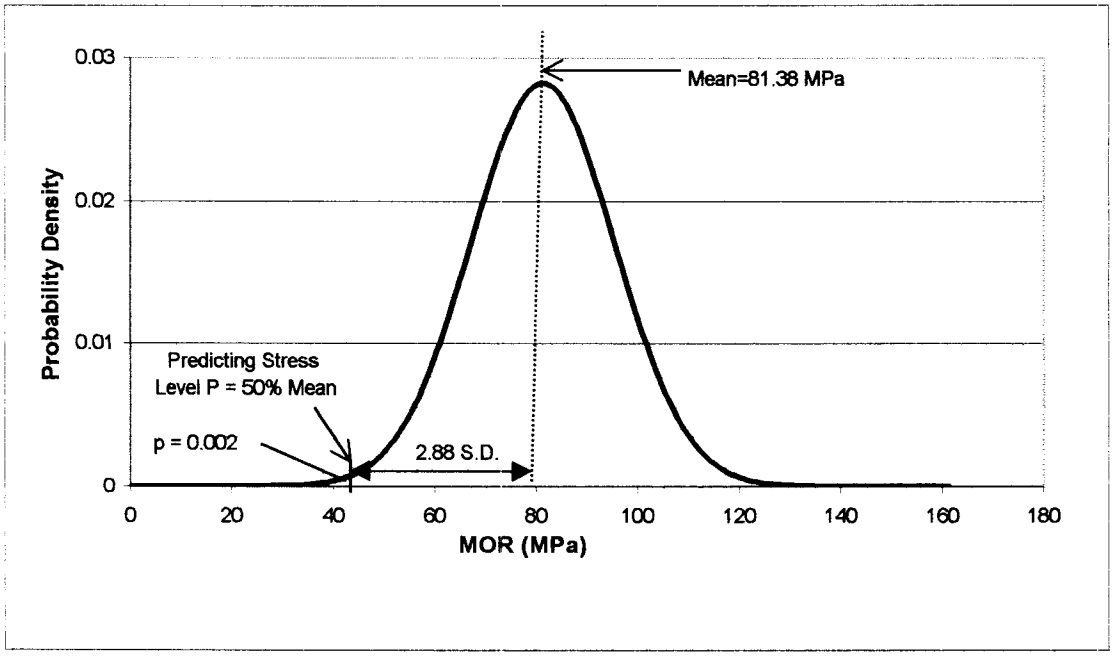

FIG. 4 Normal distribution of modulus of rupture (MOR) of finger-joints from Makore.

stress the prediction was made (Porter et al. 1972; Dedhia and Wood 1980). Two stress levels, 50% and 70% of mean ultimate bending strength, were selected for predicting the finger-joint MOR.

Predicting at stress level of 70% of mean MOR.—Prediction at 70% of mean ultimate bending strength was chosen as a value around the mean proportional limit stress of each species which was about 67%, 75%, and 76% of the mean ultimate stress of Obeche, Makore, and Moabi, respectively. A study by Strickler et al. (1970) had also shown that bending proof loads between 60 and 90% of the expected ultimate strength did not significantly reduce the strength of end-jointed Douglas-fir, indicating the general safety of the prediction at 70% of ultimate stress. Strickler (1980) also reported that a proof load is nondestructive of all pieces meeting minimum strength requirements.

Predicting at stress level of 50% of mean MOR.—For practical application, the lower stress level selected for the prediction was based on the proportion of samples expected to break during stress application. Exclusion limit for the targeted 50% stress level was calculated, from the normal distribution of each set of test data (Fig. 4), representing the proportion of samples expected to break under stress application. The predicting stress level, Q, was related to the mean ultimate stress, μ, the standard deviation, σ, and the standard normal variable, z, as follows:

$$Q = \mu - z \cdot \sigma \qquad (1)$$

Expressing the standard deviation as the product of the mean ultimate stress, μ, and coefficient of variation, CV, and also expressing the stress level as a fraction, k, of the mean ultimate stress, Eq. (1) could be rewritten as

$$k\mu = \mu - z \cdot \mu CV$$

from which

$$z = (1 - k)/C \cdot V \qquad (2)$$

Thus the exclusion limits corresponding to the 50% stress level for the three species were obtained from the normal distribution table, using the standard normal variable, z, calcu-

lated from Eq. (2). These came to about 0.02% for Obeche, 0.20% for Makore, and 3.5% for Moabi, and therefore were considered reasonably acceptable. A 50% of ultimate stress used was also to ensure that a reasonable number of acoustic emissions could be recorded for the analysis. The test results later showed that, generally, fewer AEs were emitted by most specimens of Obeche until 50% of ultimate stress was reached, whereas in Makore and Moabi, AEs were observed comparatively earlier. This explains the difference between the number of specimens tested and those analyzed for each species as indicated in the tables of results.

Theoretical considerations on AEs.—Dunegan and Harris (1969) assumed that the AE count rate would be proportional to the rate of increase of the volume of metal producing the AE. This led to the prediction that cumulative AE pulses at any time during testing would be proportional to the fourth power of the stress intensity factor associated with the flaw at the time. According to Hartbower et al. (1972), Ono (1973), and Suzuki and Schniewind (1987), however, the release rate of fracture energy, G, in plane stress of isotropic materials is related to the stress intensity factor, K, by

$$G = K^2/E \tag{3}$$

where E is Young's modulus.

Onogami et al. (1979) also reported that cumulative AE count, N, is related to the stress intensity factor, K, by

$$N \propto K^2 \tag{4}$$

The stress intensity factor, K, is known to be proportional to the applied stress, P, as follows

$$K \propto P \tag{5}$$

indicating that cumulative AE count is related to the applied stress as follows

$$N \propto P^2$$

This implies that,

$$N = aP^2 \tag{6}$$

where a = constant.

Sato et al. (1985), however, found that although their test data followed Eq. 6, it could best be represented as follows

$$N = aP^2 + b \tag{7}$$

where a = regression coefficient of the cumulative AE count versus applied stress curve, and b = coefficient relating to the Kaiser effect.

The importance of the relationship between applied stress and cumulative AE lies in the possibility of estimating MOR nondestructively using AEs (Hartbower et al. 1972). The regression of N on P for the finger-jointed specimens under the present study (Fig. 5) followed Sato's et al. (1985) regression function expressed by Eq. 7.

AE generation from the different profiles and lumber species.—The cumulative AE count versus applied stress curves (Fig. 5) and the results presented in Table 3 showed that, generally, AE started earlier in specimens of profiles F1 and F3 than those from profile F2 for finger-joint specimens of Obeche. For profile F2 of Obeche, AE activity began at about 53% of mean MOR. For specimens of Makore and Moabi, however, AE began at stress levels between 20% and 23% of mean MOR for the three profile types. Two tendencies seemed observable on the AE patterns from all profiles of the three species (quite distinct on profile F2 in Fig. 5). The AEs increased slowly after stress application until just around the mean proportional limit stress (Table 3) when they increased rapidly until failure occurred at comparatively lower stress levels for profiles F1 and F3 than for profile F2. Curves of profile F2 were of lower curvature (flatter) than those of profiles F1 and F3, especially for Makore and Moabi, possibly stemming from the less rapid increase in AE generation. A more rapid and early AE activity has been reported to be indicative of a weaker specimen (Pollock 1971; Noguchi et al. 1986, 1992; Beall and Wilcox 1987). The patterns of AEs for all profile types of the three species seemed to be indicative of the fact that finger-joints from profile F2 were stronger (Table 3) and more

TABLE 3. *Mean stresses and ratios of stresses at first AE count to modulus of rupture for finger-joints from Obeche, Makore, and Moabi.*

Species	Profile type	Mean stress at 1st AE count (MPa)	Mean modulus of rupture (MPa)	Mean proportional limit stress (MPa)	*Ratio of stress at 1st AE to MOR (%)	Mean regression coefficient, *a*, at 50% prediction level	Mean regression coefficient, *a*, at 70% prediction level
OBECHE	F1	14.01	42.31	28.01	33	0.046 (0.004 – 0.113)	0.054 (0.007 – 0.129)
	F2	22.40	45.97	29.50	53	0.012 (0.003 – 0.025)	0.016 (0.005 – 0.035)
	F3	12.52	40.47	28.73	29	0.028 (0.004 – 0.067)	0.043 (0.008 – 0.104)
	ALL F	15.70	42.56	28.72	38	0.028 (0.003 – 0.113)	0.037 (0.005 – 0.129)
MAKORE	F1	17.11	73.76	55.20	21	0.032 (0.007 – 0.124)	0.030 (0.003 – 0.130)
	F2	16.80	97.05	71.42	21	0.012 (0.007 – 0.027)	0.020 (0.005 – 0.050)
	F3	16.10	74.04	56.01	20	0.021 (0.007 – 0.055)	0.032 (0.004 – 0.100)
	ALL F	16.62	81.00	60.62	21	0.022 (0.007 – 0.124)	0.029 (0.003 – 0.130)
MOABI	F1	15.10	59.45	45.40	23	0.028 (0.005 – 0.150)	0.042 (0.009 – 0.170)
	F2	13.90	88.00	64.82	21	0.021 (0.005 – 0.070)	0.021 (0.010 – 0.060)
	F3	15.30	54.29	43.52	23	0.029 (0.005 – 0.092)	0.051 (0.011 – 0.139)
	ALL F	14.91	66.69	50.91	22	0.026 (0.005 – 0.150)	0.039 (0.009 – 0.170)

*Ratio calculated using mean MOR of all profiles of each species (i.e. ALL F). Values in parentheses are ranges of the regression coefficients, *a*.

efficient than those from profiles F1 and F3. This result agreed with earlier results reported on finger-joints from the same hardwoods (Ayarkwa et al. in press). For the three hardwoods studied, AEs from finger-joints from the low-density Obeche began comparatively later, about 38% of mean MOR, than those from the medium-density Makore and the high-density Moabi, which began at 21% and 22% of mean MOR, respectively (Table 3). Emission from Obeche, however, appeared to be more rapid after start of emission compared with those from Makore and Moabi. The late start of AE activities for finger-joints from Obeche may possibly be due to their comparatively higher joint efficiencies (Ayarkwa et al. in press). The more rapid AE generation may have resulted from the low density, low MOE, and larger breaking deflection of Obeche. This also agreed with the properties of finger-joints from the three hardwoods already reported by Ayarkwa et al. (in press). The different patterns of AE generated appeared to correlate well with the MOR of the specimens as suggested by Sato et al. (1985).

Predicting MOR.—An attempt was made to evaluate the possibility of using AE patterns to predict finger-joint MOR by plotting for each specimen the cumulative AE count versus applied stress curves up to 50% and 70% of mean ultimate stress of finger-joints of each species (Fig. 5). The function in Eq. 7 was fit to each curve and the regression coefficient, *a,* was determined. Mean values of the regression coefficients, *a,* summarized in Table 3, indicated that the lower the regression coefficient, *a,* the stronger the finger-joint, for all finger profiles studied for each species.

For the specimens tested for each finger profile, and for the combined data for all profiles of each species, the destructive parameter MOR was correlated to the regression coefficient, *a,* for both the 50% and 70% prediction stress levels. The distribution of the data points in all cases indicated a non-linear relationship between the two variables. Using the least-squares regression analysis, the log-

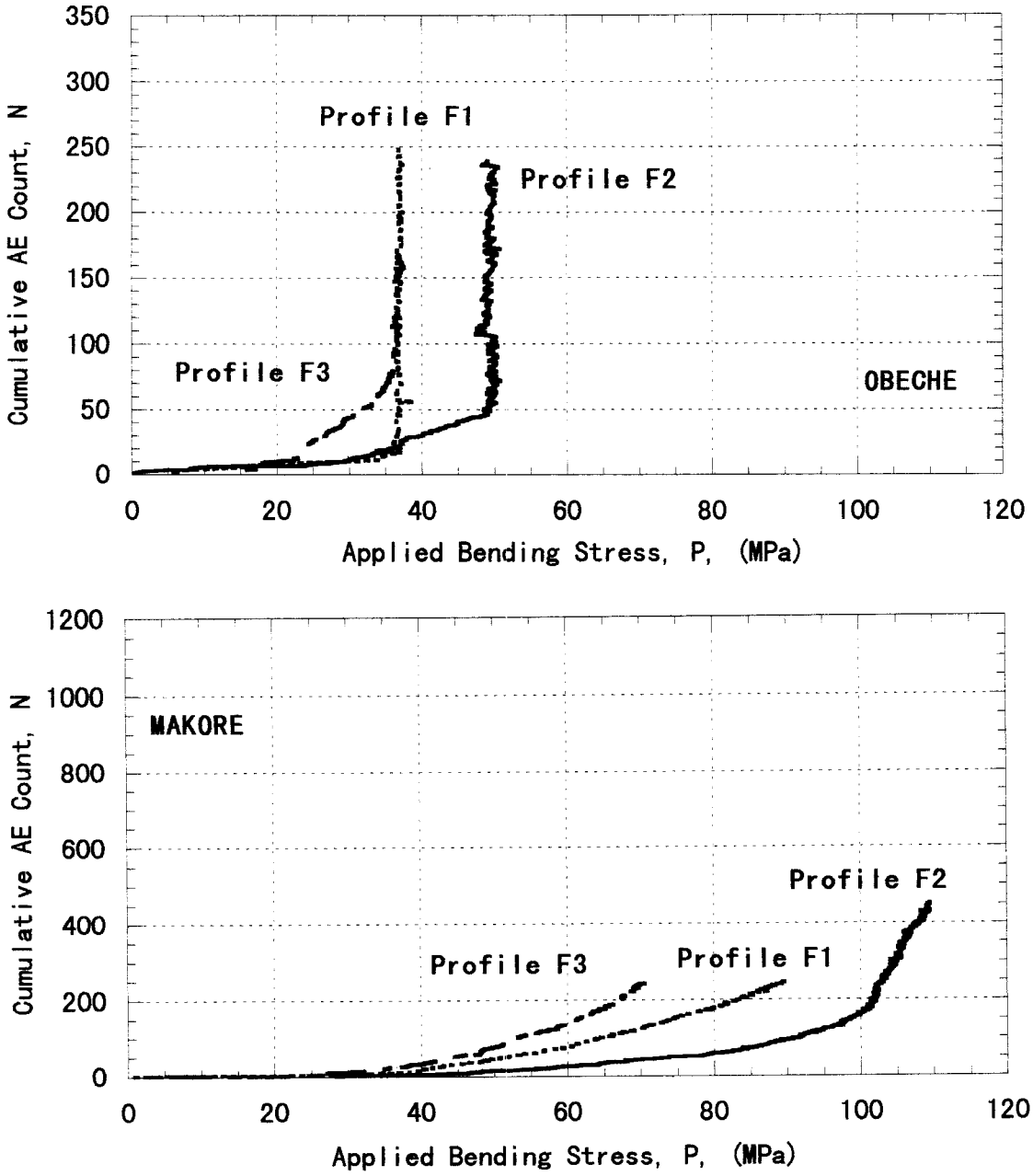

FIG. 5(a) Relationship between cumulative AE count and applied bending stress for typical Obeche finger-joints of three profile types. (b) Relationship between cumulative AE count and applied bending stress for typical Makore finger-joints of three profile types.

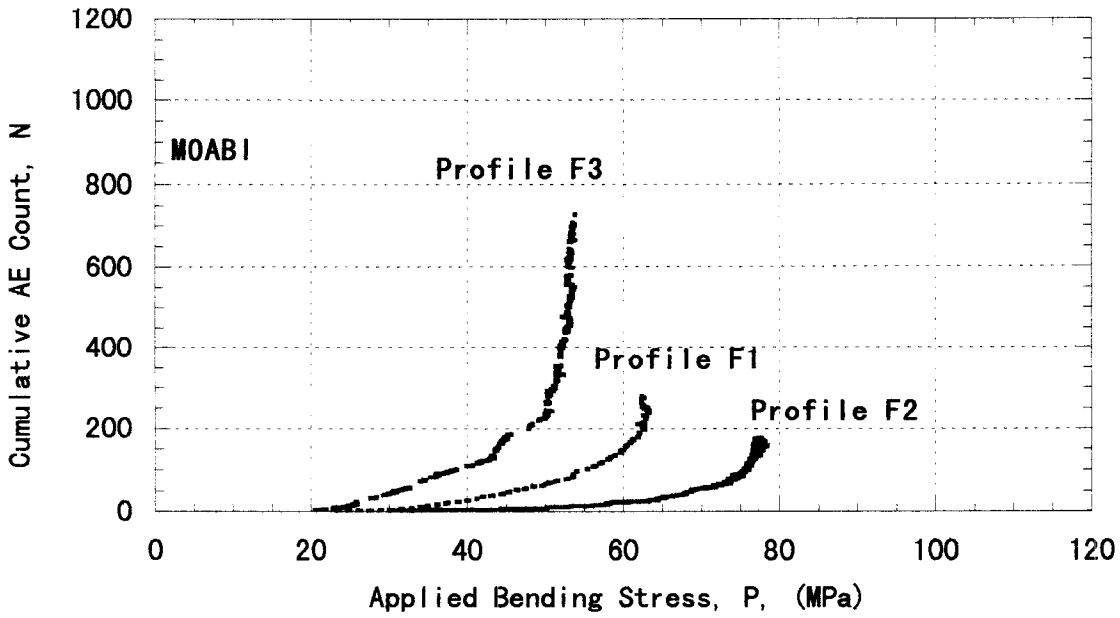

FIG. 5(c) Relationship between cumulative AE count and applied bending stress for typical Moabi finger-joints of three profile types.

arithmic function (Eq. 8) was observed to be the best-fit function.

Logarithmic function:

$$f = c \ln(a) + d + \epsilon \quad (8)$$

where f = MOR of specimen (MPa). a = regression coefficient from cumulative AE count versus applied stress curve. c, d = regression coefficients for logarithmic function. ϵ = residual error.

Absolute percentage error.—The scatter of the points on plots of MOR against the regression coefficient, a, was assumed to stem from errors of predicting the MOR. Therefore absolute percentage error for each prediction made using the developed regression models was calculated using the relationship

$$\text{Absolute percentage error (\%)} = \frac{|\text{predicted MOR} - \text{actual MOR}|}{\text{actual MOR}} \times 100 \quad (9)$$

Mean absolute percentage errors were calculated for each finger profile of each species, and for the combined data for all profiles of each species.

RESULTS AND DISCUSSION

Mean stresses and percentage ratios of stresses at start to stresses at completion of AEs for the finger-jointed specimens analyzed under the present study, are presented in Table 3. Correlation coefficients as well as mean absolute percentage errors obtained for the predictions of MOR are presented together in Table 4 for the different finger profiles of each species. In Table 5 are also presented the regression parameters and mean absolute percentage errors obtained for the combined data for all the profiles of each species, for the 50% and 70% predicting stress levels. The significance of the regression models developed for the combined data for each species was tested (at $\alpha = 0.01$) and is indicated in Table 5. Results of a one-way ANOVA performed (at $\alpha = 0.05$) to verify whether the prediction errors obtained using the 50% and 70% stress levels were statistically similar, and also whether prediction errors obtained for the different species

TABLE 4. *Summary of parameters for the regression of MOR on regression coefficient, a,* of cumulative AE count versus applied stress curve for three finger profiles of Obeche, Makore, and Moabi.

Species	Profile type	Correlation coefficients* from prediction at		#Mean absolute percentage errors from prediction at	
		50%	70%	50%	70%
OBECHE	F1	0.50 (n = 10)	0.54 (n = 17)	7.99 [5.79]	7.90 [5.35]
	F2	0.47 (n = 11)	0.29 (n = 12)	6.65 [6.23]	6.07 [6.15]
	F3	0.28 (n = 18)	0.63 (n = 28)	9.56 [8.17]	8.59 [6.70]
MAKORE	F1	0.59 (n = 24)	0.60 (n = 24)	7.25 [5.27]	7.73 [5.37]
	F2	0.20 (n = 25)	0.50 (n = 27)	8.97 [11.84]	7.73 [9.98]
	F3	0.37 (n = 30)	0.42 (n = 30)	9.51 [8.57]	9.48 [8.10]
MOABI	F1	0.73 (n = 25)	0.76 (n = 25)	12.51 [9.69]	12.33 [8.82]
	F2	0.59 (n = 22)	0.42 (n = 22)	6.61 [9.18]	4.48 [3.14]
	F3	0.50 (n = 26)	0.38 (n = 30)	6.96 [4.32]	10.76 [8.21]

n = sample size analyzed. Values in square brackets are standard deviations.
# Denotes absolute percentage error calculated from Eq. (9). * Difference between sample size tested and that analyzed mainly due to insufficient count of AE, with 5, 3, and 5 specimens excluded from Obeche, Makore, and Moabi, respectively due to failure outside finger-joint.

were statistically similar, are presented in Tables 6 and 7. Regression diagrams of MOR on static bending modulus of elasticity (MOE), for the same finger-jointed specimens are shown in Fig. 6 for comparison.

The results showed negative correlation between MOR and the regression coefficient, *a,* for all the regressions (Table 5). This indicated that as the regression coefficient, *a,* increased, MOR decreased, and vice versa. Between the 50% and the 70% predicting stress levels, correlation coefficients obtained for the regressions seemed higher for the 70% than for the 50% stress level, for all the species studied (Tables 4 and 5). Among the three finger profiles studied for each species, there seemed to be no clear advantage of one over the others in terms of correlation coefficients (Table 4), for both the 50% and the 70% predicting stress levels. This might be due to the wide variation in the results obtained for each finger profile, possibly resulting from the fewer number of test specimens analyzed. However, profile F1 appeared to have resulted in generally the highest correlation coefficients than profiles F2 and F3. The correlation coefficients obtained for the different finger profiles were not very high, ranging between 0.20 and 0.76 for the different finger profiles (Table 4) and between 0.43 and 0.70 for the combined data for each species ranging between (Table 5). This indicated that much of the total variation was not accounted for by each of the regressions. However, the tests were statistically highly significant ($\alpha = 0.01$), indicating valid regressions for the combined data (Table 5). Significant regression results suggest that the logarithmic model assumed adequately explains the relationship between MOR and the regression coefficient *a.* The range of correlation coefficients obtained under the present study was reasonably comparable with that obtained for the regression of dynamic MOE on finger-joint ultimate tensile strength for Obeche, Makore and Moabi, ranging between 0.24 and 0.74 (Ayarkwa et al. in press).

For the combined data for each species, mean absolute percentage errors obtained for the 70% prediction stress level of 9.57%, 10.67%, and 17.41% for Obeche, Makore, and Moabi, respectively, appeared comparatively lower than those for the 50% prediction stress level of 10.24%, 12.25%, and 21.19% (Tables 4 and 5). However, results of the ANOVA to verify whether the prediction errors obtained at the two stress levels were the same, showed that F-values obtained for each of the three species were less than the critical values (Table 6). The null hypotheses could therefore not be rejected, indicating that mean absolute prediction errors at the two stress levels were statistically similar ($\alpha = 0.05$). The results further showed for both the 50% and the 70% stress levels that, generally, higher accuracy

TABLE 5. *Summary of parameters for the regression of MOR on regression coefficient, a, of cumulative AE count versus applied stress curve for combined data from three profiles for each of Obeche, Makore, and Moabi.*

Species	Prediction level	No. of specimens analyzed	Linear regression model	Correlation coefficient	Significance of model at 1%	Mean absolute % error#
OBECHE	50%	39	$f = -3.972\text{Ln}(a) + 25.401$	0.47	*	10.24 (6.99)
	70%	57	$f = -3.274\text{Ln}(a) + 29.001$	0.56	*	9.57 (6.12)
MAKORE	50%	79	$f = -8.581\text{Ln}(a) + 46.664$	0.55	*	12.25 (9.63)
	70%	81	$f = -12.544\text{Ln}(a) + 36.195$	0.70	*	10.67 (8.71)
MOABI	50%	70	$f = -9.946\text{Ln}(a) + 28.059$	0.43	*	21.19 (11.42)
	70%	77	$f = -18.402\text{Ln}(a) + 3.395$	0.70	*	17.41 (11.25)

f = MOR; a = regression coefficient of cumulative AE count versus applied stress curve. Values in parentheses are standard deviations. * Denotes statistically significant at 1% level. # Denotes absolute percentage error calculated from Eq. (9).

TABLE 6. *One-way ANOVA for mean prediction errors at 50% and 70% stress levels for Obeche, Makore, and Moabi.*

Source of variation	df	F-value	F_{crit}	P-value
Between 50% and 70% stress levels				
OBECHE	1	0.24	3.95	0.6276 (NS)
MAKORE	1	1.16	3.90	0.2823 (NS)
MOABI	1	3.90	3.91	0.0501 (NS)

NS denotes not significantly different at 5% level.

was obtained when MOR was predicted from the models developed for specimens from profile F2 than from profiles F1 and F3 (Table 4) for Obeche and Moabi. Finger profile F2 was comparatively stronger (Table 3), and has been reported to be the most efficient profile among the three profiles studied (Ayarkwa et al. in press), seemingly indicating that as the quality of the finger-joints reduced, the accuracy of predicting MOR also reduced. This also agreed with Porter et al. (1972) and Dedhia and Wood (1980), who indicated that the accuracy of predicting finger-joint strength from AE depended on the nature of the joint. The decreased accuracy for the less efficient finger profiles F1 and F3 may be attributable partly to spurious acoustic signals generated by the poor-quality joints loosening up. These might have led to an underestimation of the true MOR of the specimens. Among the three species studied, prediction error appeared to increase with wood density, increasing from the low-density Obeche through the medium-density Makore to the high-density Moabi, for both the 50% and 70% predicting stress levels. Results of the one-way ANOVA (Table 7a) showed that differences in mean prediction errors obtained for the different species were statistically significant ($\alpha = 0.05$), at both prediction stress levels. The multiple comparison of the means showed that whereas mean prediction errors obtained for Obeche and Moabi and also for Makore and Moabi were statistically different, those for Obeche and Makore were not different (Table 7b). The apparent increase of prediction error with wood density may be due to the increase in variability of

TABLE 7A. *One-way ANOVA for mean prediction errors for Obeche, Makore, and Moabi at 50% and 70% stress levels.*

Source of variation	df	F-value	F_{crit}	P-value
Between species				
50% stress level	2	20.76	3.05	0.0000 (S)
70% stress level	2	14.84	3.04	0.0000 (S)

S denotes significantly different at 5% level.

TABLE 7B. *Multiple comparison of mean prediction errors at 50% and 70% stress levels for Obeche, Makore, and Moabi.*

Species	Mean prediction errors at stress level of 50%	70%
OBECHE	10.24a	9.57a
MAKORE	12.25a	10.67a
MOABI	21.19b	17.41b

Mean prediction errors with the same letter within a column are not significantly different at 5% level.

MOR and hence joint efficiencies with increase in wood density already reported on finger-joints from the three species (Ayarkwa et al. in press). The greatest variability in finger-joint MOR reported on the high-density Moabi was attributed to poor gluability, possibly stemming from low porosity, poor wettability, and the likely presence of extractives in excess amount in the wood. The decreased accuracy may have resulted from spurious acoustic signals generated by the poorly jointed fingers sliding over each other, which might also have led to an underestimation of the true MOR of the specimens. The accuracy achieved for the prediction of MOR under the present study of between ±10% and ±21 for both the 50% and 70% stress levels, may be considered as reasonably acceptable, considering the level of accuracy achieved under other nondestructive

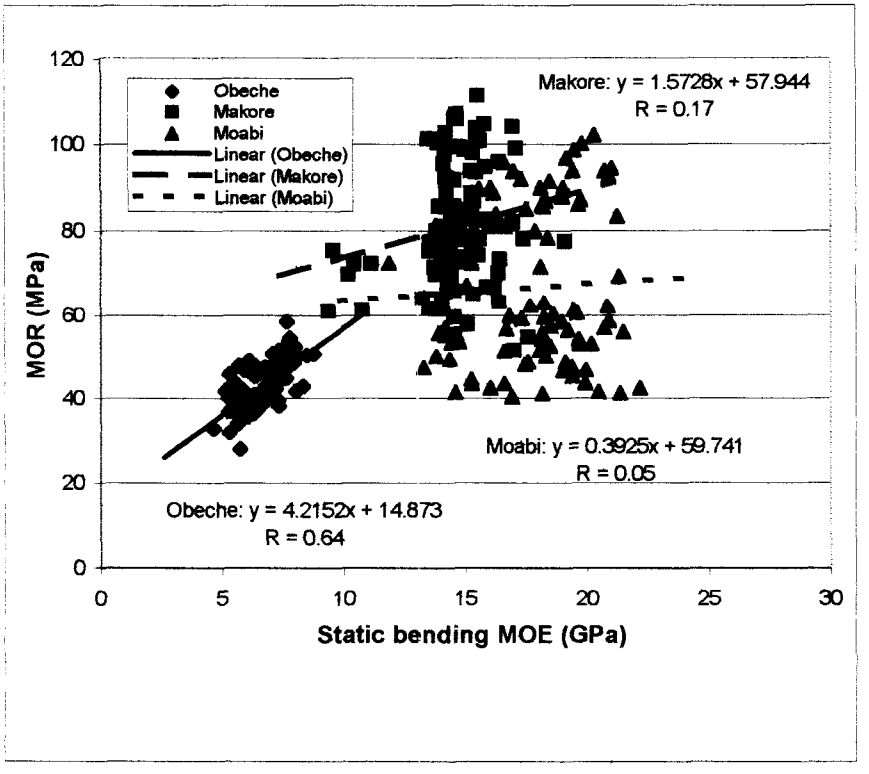

FIG. 6 Regression of modulus of rupture (MOR) on static bending modulus of elasticity (MOE) of finger-joints from Obeche, Makore, and Moabi.

prediction methods for some wood properties. Kollman and Krech (1960), for example, obtained MOEs from vibration test of oak and spruce, 14% and 19% increases, respectively over static test values; and these differences were considered as small and negligible in the opinion of the authors. Ayarkwa et al. (1999) also measured MOE by the longitudinal vibration technique, of large specimens of Obeche, Makore, and Moabi, and obtained values that were 19%, 6%, and 12%, respectively higher than static bending MOE values, and considered reasonably acceptable.

With the similarity of MORs predicted at the 50% and 70% prediction stress levels for each of the three species as basis, the lower stress level of 50% ultimate stress, which might break small proportions of the test specimens under proof loading is recommended as the better option for predicting MOR. However, for Obeche finger-joints, slightly higher prediction stress level would ensure that reasonably sufficient AE counts were emitted for subsequent analysis.

The basis of machine stress grading lies in establishing a statistical correlation between the stiffness of lumber (MOE) and its MOR. It was therefore of interest to compare this acoustic emission procedure of predicting MOR with the MOR-MOE correlation technique. The results shown in Fig. 6 gave ample evidence that correlation coefficients of 0.17 and 0.05 obtained for finger-joints from Makore and Moabi, respectively under the MOR-MOE correlation would be of little use for the material in this study. Thus the AE monitoring appears to hold greater potential for nondestructively predicting MOR of finger-joints from the three tropical African hardwoods.

CONCLUSIONS

The following conclusions can be drawn from the results of the study. Although correlation coefficients obtained for the regressions under the present study were not very high, they were comparatively higher than those obtained under the MOR-static MOE correlation, seemingly indicating superior performance advantage. The regression models developed for the combined data were all statistically highly significant ($\alpha = 0.01$), suggesting that a logarithmic model adequately explains the relationship between MOR and the regression coefficient, *a*. The results also showed that measuring AE up to 50% of mean ultimate stress predicted MOR just as accurate as measuring up to 70% of ultimate stress, justifying the choice of the lower stress level as the better option for predicting MOR. The developed models also seemed sensitive to the quality of the finger-joint, as the accuracy of predicting MOR seemed to decrease as the efficiency of the finger-joint decreases.

The results of the study have given an indication that this acoustic emission monitoring procedure could be useful for predicting MOR of finger-joints from the three tropical African hardwoods.

ACKNOWLEDGMENTS

The authors wish to acknowledge the contributions of Aichi Timber Industries Limited and Iida Industrial Company Limited for helping in the preparation of the finger-joint specimens. We also thank Oshika Shinko Company Limited for supplying glue for the study.

REFERENCES

AMERICAN SOCIETY FOR TESTING AND MATERIALS. (ASTM). 1994. Standard method of static tests of timber in structural sizes. ASTM D198-84. ASTM, West Conshocken, PA.

ANSEL, M. P. 1982. Acoustic emission from softwood in tension. Wood Sci. Technol. 16(1):35–58.

AYARKWA, J., Y. HIRASHIMA, AND Y. SASAKI. 1999. Predicting static bending modulus of elasticity of tropical African hardwoods from density using a model based on longitudinal vibration. Ghana J. Forestry 8(2000):1–8.

———, ———, ———. 2000. Predicting tensile properties of finger-jointed tropical African hardwoods using longitudinal vibration. Ghana J. Forestry 9:(in press).

———, ———, ———. 2000. Effect of finger geometry and end pressure on the flexural properties of finger-jointed tropical African hardwoods (in press). Forest Prod. J. 50(11/12).

BEALL, F. C., AND W. W. WILCOX. 1987. Relationship of

acoustic emission during radial compression to mass loss from decay. Forest Prod. J. 37(4):38–42.

BEAULIEU, C., C. VERREAULT, C. GOSME, AND M. SAMSON. 1997. Experimental assessment of the effect of length on the tensile strength of structural finger-joined lumber. Forest Prod. J. 47(10):94–100.

BODIG, J., AND B. A. JAYNE. 1982. Mechanics of wood and wood composites. Van Nostrand Reinhold Company. New York, N.Y. Pp. 247–269; 645–650.

CHRISTENSEN, R. H. 1962. Cracking and fracture in metals and structures. Crack Propagation Symposium, Coll. Aeron., Cranfield, England. Pp. 326–374.

DEBAISE, G. R., A. W. PORTER, AND R. E. PENTONEY. 1966. Morphology and mechanics of wood fracture. Mater. Res. Stand. 6(10):493, 499.

DEDHIA, D. D., AND W. E. WOOD. 1980. Acoustic emission analysis of Douglas-fir finger-joints. Mater. Eval. November 1980:28–32.

DUNEGAN, H., AND D. HARRIS. 1968. Acoustic emissions a new nondestructive testing tool. Lawrence Radiation Lab., Livermore, CA. UCRL-70750.

———. 1969. Ultrasonics. ULTRA 7:160–166.

FISETTE, P. R., AND W. W. RICE. 1988. An analysis of structural finger-joints made from two northeastern species. Forest Prod. J. 38(9):40–44.

HARTBOWER, C. E., W. E. REUTER, C. F. MORAIS, AND P. P. CRIMMINS. 1972. Use of acoustic emission for the detection of weld and stress corrosion cracking. ASTM Spec. Tech. Pub. 505:187–221.

HONEYCUTT, R., C. SKAAR, C., AND W. SIMPSON. 1985. Use of acoustic emissions to control drying rate of red oak. Forest Prod. J. 35(1):48–50.

JAPANESE INDUSTRIAL STANDARDS. 1977. Methods of test for wood. JIS Z 2101. Tokyo, Japan.

KNUFFEL, W. E. 1988. Acoustic emission as strength predictor in structural timber. Holzforschung 42(1988): 195–198.

KOHLER, G. 1981. Finger-jointing of unseasoned sawn timber for pallet manufacture. Holz-Zentralblatt 107 (130):2015–2016.

KOLLMAN, F., AND H. KRECH. 1960. Dynamic measuring of elastic wood properties and damping. Holz Roh-Werkst. 2:41–45.

LEMBKE, C. A. 1977. Finger-jointing increases value 5700%. Australian Forest Ind. J. 43(1):5–11.

NOGUCHI, M., K. NISHIMOTO, Y. IMAMURA, Y. FUJII, S. OKUMURA, AND T. MIYAUCHI. 1986. Detection of very early stages of decay in western hemlock wood using acoustic emissions. Forest Prod. J. 36(4):35–36.

———, R. ISHI, Y. FUJII, AND Y. IMAMURA. 1992. Acoustic emission monitoring during partial compression to detect early stages of decay. Wood Sci. Technol. 26(4): 279–287.

OFOSU-ASIEDU, A., J. M. NANI-NUTAKOR, AND J. AYARKWA. 1996. Kumasi base-line survey - data collection for a finger jointing plant. Research Report of the Forestry Research Institute of Ghana, Kumasi, Ghana. Pp. 1–3.

ONO, K. 1973. Present studies on acoustic emission for iron and steel. Iron and Steel 59:1338–1359.

ONOGAMI, M., K. YAMAGUCHI, H. NAKASA, K. SANO, E. ISONO, AND T. WATANABE. 1979. Acoustic emission - Bases and applications. Japan Corona Pub. Co. Pp. 125.

POLLOCK, A. A. 1971. Acoustic emission methods of NDT. Brit. J. NDE 13:85–89.

PORTER, A. W. 1964. On the mechanics of fracture in wood. Ph.D. Thesis, Suny College of Forestry. Syracuse, NY.

———, M. L. EL-OSTA, AND D. J. KUSEC. 1972. Prediction of failure of finger-joints using acoustic emissions. Forest Prod. J. 22(9):74–82.

PRAH, E. A. 1994. Environment and recovery in industrial processing of timber. Seminar on "The Environment and the Utilization of Wood Waste". Assoc. Ghana Industries and the Friedrich Naumann Foundation. Kumasi, Ghana. Pp. 5–10.

RICE, R. W., AND C. H. SKAAR. 1990. Acoustic emission patterns from the surface of red oak wafers under transverse bending stress. Wood Sci. Technol. 24(2):123–129.

SAMSON, M. 1985. Potential of finger-joined lumber for machine stress-rated lumber grades. Forest Prod. J. 35(7/8):20–24.

SATO, K., T. OKANO, L. ASANO, AND M. FUSHITANI. 1985. Application of AE to mechanical testing of pages 240–243 wood. Proc. 2nd Int. Conf. on Acoustic Emission. Lake Tahoe, CA.

STRICKLER, M. D. 1980. Finger-jointed dimensioned lumber-Past, present and future. Forest Prod. J. 30(9):51–56.

———, R. F. PELLERIN, AND J. W. TALBOTT. 1970. Experiments in proof loading structural end-jointed lumber. Forest Prod. J. 20(2):29–35.

SUZUKI, M., AND A. P. SCHNIEWIND. 1987. Relationship between fracture toughness and acoustic emission during cleavage failure in adhesive joints. Wood Sci. Technol. 21:121–130.

ULASOVETS, V. G., AND L. A. MAKEROVA. 1988. Standardizing factors in the manufacture of single-layer parquet panels. Derevoobrabatyvayushchaya-Promyshlennost 11:14–15.